EBioMedicine 49 (2019) 118–132

Contents lists available at ScienceDirect

EBioMedicine

journal homepage: www.elsevier.com/locate/ebiom

Research paper

Rab8 GTPase regulates Klotho-mediated inhibition of cell growth and progression by directly modulating its surface expression in human non-small cell lung cancer

Bo Chen[a,b], Shuhong Huang[c], Thomas R. Pisanic, II[b], Alejandro Stark[d], Yong Tao[e], Bei Cheng[f], Yue Li[a], Yunyan Wei[g], Weihong Zhao[a], Tza-Huei Wang[b,d,e,h], Jianqing Wu[a,*]

[a] Jiangsu Provincial Key Laboratory of Geriatrics, Department of Geriatrics, Jiangsu Province Hospital, the First Affiliated Hospital of Nanjing Medical University, 300 Guangzhou Road, Nanjing, Jiangsu 210029, China
[b] Johns Hopkins Institute for NanoBioTechnology, Johns Hopkins University, Baltimore, Maryland 21218, United States
[c] Institute of Basic Medicine, Shandong Academy of Medical Sciences, Jinan, Shandong 250000, China
[d] Department of Biomedical Engineering, Johns Hopkins University School of Medicine, Baltimore, Maryland 21205, United States
[e] The Sidney Kimmel Comprehensive Cancer Center, Johns Hopkins University School of Medicine, Baltimore, Maryland 21287, United States
[f] Department of Radiology and Radiological Science, Johns Hopkins University School of Medicine, Baltimore, Maryland 21205, United States
[g] Department of Respiration, Nanjing First Hospital, Nanjing Medical University, Nanjing, Jiangsu 210006, China
[h] Department of Mechanical Engineering, Johns Hopkins University, Baltimore, Maryland 21218, United States

ARTICLE INFO

Article history:
Received 21 June 2019
Revised 18 October 2019
Accepted 22 October 2019
Available online 6 November 2019

Keywords:
Rab8
Klotho
Surface expression
Non-small cell lung cancer
Wnt signaling
Cell phenotype

ABSTRACT

Background: The *klotho* (KL) gene is an anti-aging gene that has recently been shown to also function as a general tumor suppressor. However, there is currently only limited information regarding the potential molecular signals for regulation of Klotho without identifying precise molecular mechanisms or interactions.

Methods: We performed a mass spectrometry (MS) assay to screen candidate proteins complexed with Klotho derived from immunoprecipitation in human non-small cell lung cancer (NSCLC) cells, and identified Rab8 to be the protein that most prominently interacts with Klotho. We further investigated whether Rab8 can regulate trafficking of Klotho and which process it would modulate using surface biotinylation assay, immunofluorescence and fluorescence ratio microscopy. Furthermore, we explored whether Rab8 is involved in Klotho-mediated function in NSCLC, and verified the results which we found *in vivo* using xenograft mouse model.

Findings: We report discovery of Rab8 as a Klotho-interacting protein that acts as a critical modulator of Klotho surface expression in human NSCLC. In particular, we report that Rab8 is co-localized and associated with Klotho, and Klotho trafficking is regulated by Rab8. Moreover, we found that Rab8 modulates surface levels of Klotho via a post-biosynthetic pathway, as opposed to an endocytic pathway. Furthermore, we demonstrate that Rab8 is involved in Klotho-mediated regulation of cell proliferation, migration, invasiveness, epithelial-mesenchymal transition (EMT), and Wnt-β-catenin signaling in NSCLC. Additionally, Rab8 overexpression was also found to increase Klotho-mediated inhibition of NSCLC tumorigenesis *in vivo*.

Interpretation: Overall, our findings suggest that Rab8 GTPase can regulate Klotho-mediated inhibition of Wnt signaling activity by modulating translocation of Klotho onto the cell surface, which in turn affects Klotho-mediated inhibition of cell proliferation, migration and invasiveness in NSCLC. These results have important implications for the development of new therapeutic targets, Klotho-related research in the context of NSCLC as well as other areas, and provide a working model for Rab8 function in the context of cancer and cancer biology.

* Corresponding author.
E-mail address: jwuny@njmu.edu.cn (J. Wu).

https://doi.org/10.1016/j.ebiom.2019.10.040

Research in context

Evidence before this study

The klotho (KL) gene is an anti-aging gene that has recently been shown to also function as a general tumor suppressor. However, there is currently limited information regarding the sub cellular location and trafficking of Klotho.

Added value of this study

We identified of Rab8 as a novel Klotho-interacting protein that acts as a critical modulator of Klotho surface expression in human NSCLC. We found that Rab8 modulates surface levels of Klotho via a post-biosynthetic pathway. Furthermore, we demonstrate that Rab8 is involved in Klotho-mediated regulation of cell proliferation, migration, invasiveness, epithelial-mesenchymal transition (EMT), and Wnt-β-catenin signaling in NSCLC.

Implications of all the available evidence

Our findings have important implications for the development of new therapeutic targets, Klotho-related research in the context of NSCLC as well as other areas, and provide a working model for Rab8 function in the context of cancer and cancer biology.

1. Introduction

Lung cancer is the leading cause of cancer deaths worldwide because of its high incidence and associated mortality [1]. Non-small cell lung cancer (NSCLC) accounts for over 80% of all lung carcinomas and continues to increase in incidence [2]. With a 5-year survival rate of only 10%, it remains of great importance to explore the underlying mechanisms of NSCLC in order to develop more effective therapeutic interventions.

The *klotho* gene (KL) was first identified in 1997 as an anti-aging gene. Klotho knockout mice exhibit multiple aging-related syndromes including a shorter lifespan and premature emphysema [3], while mice with increased KL expression average significantly increased life spans [4]. The *klotho* gene encodes a single-pass transmembrane protein composed of a large extracellular domain, a transmembrane domain, and a very short intracellular domain. Membrane Klotho functions as an obligate co-receptor of fibroblast growth factor 23 (FGF23) to regulate phosphate homeostasis. Previous studies also suggest that the Klotho extracellular domain (secreted Klotho) can be released into the serum and function as a circulating hormone to regulate the activity of oxidative stress, multiple growth factor receptors, ion channels and several signaling pathways such as Wnt/β-catenin, IGF-1/insulin and p53/p21 [5]. Moreover, Sato and colleagues reported that $p16^{INK4a}$ plays a role in promoting aging phenotypes through the downregulation of the expression of the Klotho [6].

Recently, multiple studies have shown that Klotho expression is widely decreased and can function as a tumor suppressor in different types of cancer, including breast [7,8], lung [9–13], pancreatic [14], ovarian [15], cervical [16], gastrointestinal [17], liver [18], kidney [19] cancers, as well as melanoma [20]. Current studies have found that Klotho activity is mainly implicated in regulating cellular signaling pathways, such as the IGF-1/insulin and Wnt/β-catenin signaling pathways, both of which are critically implicated in cancer development and progression [21,22]. Current studies have also found that the extracellular domain of Klotho can bind to multiple Wnt ligands and inhibit their ability to activate Wnt signaling. Specifically, Klotho inhibits activation of the Wnt-TCF/β-catenin signaling pathway, leading to decreased expression of target genes such as c-Myc and Cyclin D1, thereby inhibiting cancer cell development and progression [11,18,20,23–25]. We have also previously first reported the role of Klotho in the pathogenesis of human lung cancer, showing that ectopic Klotho expression can inhibit lung cancer proliferation and motility, and trigger apoptosis by modulating IGF-1/insulin signaling and the Wnt signaling pathway [11,13].

While numerous studies have demonstrated important tumor suppressor roles of Klotho, there is currently only limited information regarding the potential molecular mechanisms by which Klotho is regulated. Specifically, as a type-I membrane protein, the function of Klotho is closely related to its trafficking or subcellular location and metabolism kinetics, which have only been explored in a limited number of studies [26].

In this study, we attempted to explore the potential molecular signals for regulation of Klotho, including Klotho-interacting proteins and associated functions, and the potential subcellular location and trafficking of Klotho in NSCLC. Toward this end we perform mass spectrometry (MS) to screen candidate proteins complexed with Klotho derived from immunoprecipitation in lung cancer cells. From this analysis, we identify Rab8 to be the protein that most prominently interacts with Klotho. Rab8 is a small Ras-related GTPase, involved in protein trafficking and secretion, and mainly regulates trafficking from the trans-Golgi network (TGN) to the cell surface [27]. We thus further investigate whether Rab8 can also regulate trafficking of Klotho, as well as the processes that might modulate this regulation. Lastly, we explore whether Rab8 is involved in Klotho-mediated function in NSCLC, including regulation of the Wnt pathway, cell proliferation, colony formation, migration and invasion, and verify these results in an *in vivo* using xenograft mouse model of NSCLC.

2. Materials and methods

2.1. Antibodies and other reagents

Anti-Rab8 antibody (Abcam, ab188574, Hong Kong Ltd.). Anti-Klotho antibody (Abcam, ab181373, Hong Kong Ltd, for IHC;Santa Craz, sc-74205, for WB) Wnt3 rabbit monoclonal antibody (EPITOMICS, Cat. #1026-1, Epitomics Inc.). β-catenin antibody (Cell signaling technology, Cat. #9562, Cell signaling technology Inc.). Anti-Active-β-Catenin (Anti-ABC) antibody (clone 8E7) (Millipore, Cat. 05-665, Merckmillipore Inc.). Other reagents: Dulbecco's modified Eagle medium- high glucose (GIBCO). Fetal bovine serum (GIBCO), 0.25% trypsin (GIBCO), SYBR Green Realtime PCR Master Mix (TOYOBO, QRT-101), First Strand cDNA Synthesis Kit (TOYOBO, FSK-101), Trizol (Invitrogen, 66012), Lipofectamine® 2000 Reagent (Invitrogen, Cat. #11618-019), Opti-MEM (Invitrogen, Cat. #31985-062).

2.2. Cell culture

The human non-small cell lung cancer cell lines A549, H1299, H1650, H1975, Lu-165 and H125, human large cell lung cancer cell line H460, and human embryonic kidney (HEK) 293 cell line were purchased from the Type Culture Collection of the Chinese Academy of Sciences (Shanghai, China). All of the cell lines were cultured in DMEM supplemented with 10% FBS, at 37 °C in a humidified incubator with 5% CO_2. Upon reaching 90% confluence, cells were dissociated with 0.25% trypsin and split.

2.3. Label-free quantitative mass spectrometry

Cultured A549 cells were transfected with Flag Klotho vector. 48 h later, cells were lysed for an agarose-Flag antibody pulldown assay. The immunoprecipitates were sent for label-free quantitative mass spectrometry analysis. Some of the unpublished mass spectrometry data will be prepared for publication elsewhere. We con-

firm that there is no overlap between the mass spectrometry data used here and those submitted elsewhere.

2.4. Plasmid, siRNA, RT-PCR and transfection

Overexpression plasmids of Flag-KL and Myc/HA-Rab8, Rab8 mutants Myc/HA-Rab8Q67L and Myc/HA-Rab8T22N were subcloned into pCDNA3.1(+) expression vector (Invitrogen). Plasmids with Rab8T22N or Rab8Q67L were generated by PCR mediated site-directed mutagenesis. The C-terminal Myc/or HA epitope tag was added before the stop codon by PCR. All constructed plasmids were sequenced (Sanger).

Rab8 siRNA sequence:

Rab8 siRNA1# (siRab8-1): 5′- CGA GAA GTC CTT CGA CAA CAT -3′;

Rab8 siRNA2# (siRab8-2): 5′- CGG AAC TGG ATT CGC AAC ATT -3′;

Rab8 siRNA3# (siRab8-3): 5′- TCG CCA GAG ATA TCA AAG CAA -3′;

Rab8 siRNA negative control (siNC): 5′- ATG TTG TCG AAG GAC TTC TCG -3′.

Plasmids or siRab8 were transfected using Lipofectamine® 2000 Reagent (Invitrogen).

Quantitative RT-PCR was performed on a Bio-rad 480 (Bio-rad, USA) using SYBR Green qPCR. qRT-PCR primers as follows:

Rab8 (189 bp), sense:5′-AAAGCTGGCCCTCGACTATG-3′; antisense: 5′-CTGCTCCTCTTCTGCTGGTC-3′;

CyclinD1 (322 bp), sense: 5′- CCGCTGGCCATGAACTACCT-3′; antisense: 5′- ACGAAGGTCTGCGCGTGTT-3′;

C-myc (110 bp), sense: 5′- TCAAGAGGCGAACACACAAC −3′; antisense: 5′- GGCCTTTTCATTGTTTTCCA −3′;

Klotho (374 bp), sense: 5′ –CGACCACTTCAGGGATTACGC-3′; antisense: 5′ –GGATAGTCACCATCAATAAATACGG-3′.

2.5. Lentivirus production

The pUltra lentiviral vector was obtained from Addgene (plasmid 24,129). The human Rab8or Klotho cDNA was cloned into the XbaI-BamHI sites, downstream of the 2a peptide coding sequence, in frame with the enhanced GFP sequence, allowing for the bicistronic expression of enhanced GFP. To obtain virus, 293T cells were co-transfected with the vector plasmid (pUltra, pUltra-KL or pUltra-Rab8), the packaging plasmid psPAX2 and the envelop plasmid pMD2 G (addgene plasmids 12,259, 12,260). The titers of viral supernatants were determined by infecting 293T cells, and FACS analysis was performed.

2.6. Immunohistochemistry

We first measured the endogenous level of Klotho in NSCLC tissues and para-carcinoma tissues obtained from patients using tissue microarray analysis. Tissue microarray was purchased from Superchip (Shanghai, China). Immunohistochemistry was performed using standard procedures. Briefly, a series of deparaffinization was done with xylene and ethanol alcohol. Antigen retrieval was performed by boiling tissue slides with 0.01 mol/L citric buffer. Hydrogen peroxide was used to quench the endogenous peroxidase activity. After blocking, the sections were incubated with primary antibodies rabbit against human Klotho with work concentration 1:100, overnight at 4 °C. Corresponding biotin goat anti-rabbit IgG secondary antibodies with work concentration 1:3000, incubated 1 h at room temperature and peroxidase-conjugated streptavidin (Jackson 016-030-084), incubated 30 min at room temperature, and finally colored with diaminobenzidine (DAB). Stained slides were counterstained with formulation hematoxylin and then dehydrated with alcohol and xylene and mounted in resinous mounting media. Tissue sections stained with isotype IgG were used as controls. All slides stained with the same antibody were processed at the same time. All compared images were acquired under identical imaging parameters.

2.7. Immunoprecipitation

After protein extraction, 1 mg protein was mixed with 2ug rabbit IgG (Santa Cruz, Cat. # H270)/ or Flag (M2) antibody and 40ul Protein G Plus-Agarose (Santa Cruz, Cat. # sc-2002) at 4 °C overnight. The beads were then pelleted and washed five times with lysis buffer. After a final centrifugation, the pellet was suspended in 4 × SDS-PAGE loading buffer and boiled for 5 min prior to immunoblotting.

2.8. Immunoblotting

Equal loading samples were run on an SDS polyacrylamide gel and transferred to PVDF membranes. After blocking 1 h in 5% w/v no fat milk, 1 × TBS, 0.05% Tween-20, membranes were incubated with indicated primary antibodies overnight at 4 °C. Primary antibody bound membranes were washed 3 times in TBS-T and incubated for 1 h at room temperature with secondary antibody conjugated with horseradish peroxidase (santa cruz, sc2004) at a working concentration of 1:10,000. Immunosignals were visualized, in accordance to manufacturer's instructions, via ECL. All experiments were performed in triplicate.

2.9. RNA preparation and real-time PCR assay

Total RNA was extracted using RNA extraction kit (CoWin Bioscience, Beijing, China) and total RNA was converted into cDNA using the cDNA synthesis kit (CoWin Bioscience, Beijing, China), The qRT-PCR conditions for genes were set at 95 °C for 5 min, 95 °C for 30 s, followed by 40 cycles at 60 °C for 45 s and 72 °C for 3 min, each reaction was performed in triplicate. The expression of Rab8, cyclin D1, c-Myc and Klotho was calculated using the 2-△Ct method. Three independent experiments were performed to analyze relative gene expression.

2.10. Surface biotinylation assay

For biotinylation experiments, the cells were plated at a density of 1×10^6 cells/ml. Cell surface protein biotinylation were performed as previously described [28]. Briefly, cells were washed twice with ice-cold phosphate-buffered saline (PBS) and incubated with 300 μg/ml sulfo-N-hydroxysuccinimide-biotin (Pierce) in PBS for 45 min at 4 °C to biotinylate surface proteins. Unreacted biotin was quenched and removed with tris-buffered saline. Biotinylated cells lysed in extraction buffer (1.0% (v/v) Triton X-100, 10 mM Tris-HCl, pH 7.5, 120 mM NaCl, 25 mM KCl, 1 μg/ml leupeptin, 1 μg/ml pepstatin, 2 μg/ml aprotinin, and 0.5 mM phenylmethylsulfonyl fluoride). Extracts were clarified by centrifugation (12,000× g for 15 min), and then biotinylated proteins were isolated from cell extracts by precipitation with streptavidin-conjugated sepharose beads (Pierce). Washed beads were eluted with SDS sample buffer, and eluted proteins were separated by SDS-PAGE. For densitometric analyses, immunoreactive bands were scanned and quantitated using NIH Image J (Scion, Frederick, MD). All experiments were carried out at least in triplicate.

2.11. Immunofluorescence

A549 or H1299 cells were cultured on coverslips to appropriate density. After 48 h of transfection, cells were fixed with 4% PFA for 10 min, and then permeabilization-treated with 0.4% Triton X-100

for 10 min. After blocking in 10% normal goat serum for 60 min, slides were incubated with the primary antibody diluted in TBS for 1 h. After washing with PBS, slides were incubated with Alexa Fluor 488- or 594-conjugated secondary antibodies (1:1000 dilution) for 1 h. After washing with TBS, then sealed to a cover glass plate with VECTASHIELD (Abcam).

2.12. Surface Klotho measurement

Cells transfected with FLAG-KL/siNC or Flag-KL/siRab8 were grown on glass coverslips. 48 h after transfection, cells were fixed with 4% paraformaldehyde, then incubated with Alexa-488-conjugated M2 anti-FLAG antibody for 60 min at 37 °C to selectively label FLAG-tagged receptors on the plasma membrane. At the end of this incubation, cells were quickly washed 3 times with ice-cold PBS, and mounted with Vectashield mounting medium. The parallel control (blank) coverslips were included, in which cells were transfected with empty pCDNA3.1 vector. Cells were examined by fluorescence microscopy using appropriate filter sets to selectively detect Alexa-488, and staining intensities of each fluor in individual cells were integrated using MetaMorph software (Molecular Devices, Sunnyvale, CA). Each experimental condition was repeated at least three times. In each experiment more than 60 cells were examined at random.

2.13. Microscopic quantitative analysis

Fluorescence images were acquired by a HQ2 cool CCD camera mounted on a Nikon Eclipse TE 2000-U microscope. All of the images were collected using a 40 × objective lens. To quantitatively analyze the amount of surface to total Klotho, more than 60 cells were examined at random. A region was selected in each image and the intensity of anti-FLAG staining or GFP for each of these (ROIs) [29] was measured by the MetaMorph software (Universal Imaging Corporation, West Chester, PA). In every experiment, including TrkB-FL and all the mutants, a consistent set of acquisition parameters was used for each set of images. To calculate the level of Klotho surface fluorescence, we selected ROIs (regions of interest) in the Alexa Fluor 488 staining images, in which surface Klotho was stained with green fluorescence and 'ring-like'. The fluorescence of each ROI was measured and calculated to green signal intensity. For comparable analysis of the surface Klotho levels in siNC and siRab8 group: we used the following formula (F_{siRab8}- F_{blank})/(FsiNC- F_{blank})X100. Each experimental condition was repeated at least three times. All statistical analysis was performed using SPSS Software [30]. The results of more than three independent experiments were compiled, and the mean ± SEM was calculated.

2.14. CCK8 assay

After 24 h of transfection, 96-well plates were seeded at a cell density of 1×10^4 cells/well. At selected time course including 0 h, 24 h, 48 h, 72 h after cell attachment, 10 ul CCK-8 was added into each well containing cells and incubated 30 min before measurement at 450 nm wavelength. Every step was done according to the protocol of the CCK8 assay (Lot#EX783, Dojindo Laboratories, Tokyo, Japan). Results are presented as mean values of three replicate experiments with different passages.

2.15. Cell colony formation

A549 and H1299 cells were trypsinized, counted, plated on a 6-well plate at a starting density of 100 cells/well, incubated at 37 °C and culture medium was changed every 2 days. After incubation for 14 days, the cell colonies were fixed with 4% paraformaldehyde for 10 min and stained with crystal violet for 20 min at room temperature. Cell colonies were counted under a light microscope and photographed using a digital camera. Each sample has three independent copies.

2.16. Wound healing assay

Cells were seeded on 6-well plates at 2×10^5 cells/well and cultured for 24 h at 37 °C in a humidified, 5% CO_2 atmosphere to confluency. A sterile pipette tip was then used to scratch a straight line in each well. The cells were incubated with fresh medium (containing 2% serum) for 48 hrs and then the wound closure was quantified by measuring the remaining blank area using Image J. Assays were performed for three independent experiments.

2.17. Transwell assay

Cell suspension (200 μL at 2×10^5 cells/mL) was added to the insert of a 24-well transwell plate with 8 μm pore polycarbonate filters (Costar, Corning, NY, USA). In the lower chamber, 500 μL of DMEM containing 10% FBS was added to all groups except the control. The cells were incubated for 24 h at 37 °C in a humidified, 5% CO_2 atmosphere. Each group has three independent wells. After incubation, the medium was removed from the insert and cells in each group were scraped off with a cotton swab. The cells that had migrated to the lower surface of the membrane were fixed with 4% paraformaldehyde for 20 min and stained with 0.1% crystal violet for 5 min. Migrating cells were counted under a microscope at 200 × magnification in five random fields of view. Three independent experiments were performed.

2.18. Analysis of Klotho recycling by using fluorescence ratio microscopy

Klotho recycling assay was performed as described by Huang and colleagues [28]. A549 cells were transfected with the indicated constructs using Lipofectamine 2000 for 48 h before the recycling experiment. Cells were serum starved overnight and then incubated with anti-Flag antibody (M1, calcium sensitive) conjugated to Alexa Fluor 488 (A488-M1) at 4 °C for 30 min. Then, cells were rewarmed with DMEM at 37 °C for 30 min followed by three quick washes with cold PBS containing EDTA (1 mM) to dissociate the A488-M1 bound to un-internalized Klotho. Subsequently, cells were incubated in fresh medium containing A594-conjugated anti-Mouse IgG secondary antibody at 37 °C for 45 min to label the recycled protein with A488-M1. Then, cells were immediately fixed. Images were acquired using epifluorescence microscopy. The Alexa Fluor 594 to 488 fluorescence ratio was calculated using MetaMorph software. The mean Alexa Fluor 594 to Alexa Fluor 488 ratio of the recycling group described above is defined as E. For each experiment, two parallel control groups (data not shown) were assessed: one is the 100% surface control, cells were fixed immediately after the 30 min incubation with A488-M1 and subsequently labeled with A594-conjugated anti-mouse IgG antibody, and the mean ratio of this group designated as C; another is the 0% recycled control, cells were fixed immediately after the EDTA-stripping step and then labeled with A594-conjugated anti-mouse IgG antibody, and the mean ratio of this group is designated as Z. Thus, the percentage of recycled Klotho was calculated using the following formula: (E-Z)/(C-Z) × 100.

2.19. Animal experiments and sample collections

Male athymic nude mice (BALB/c, 4 weeks old) were obtained from Beijing Vital River Experimental Animal Technical Co., LTD. All experimental procedures involving animals in this study were

reviewed and approved by the Institutional Animal Care and Research Advisory Committee at Nanjing Medical University. The mice were housed in a local SPF experimental animal facility with a 12 h light/dark cycle and constant temperature and relative humidity (to about 50%). Two weeks later, the nude mice were inoculated with either A549 cells infected with NC, KL or KL/Rab8 virus (KL- and Rab8-co-infected). For xenograft tumor models, each nude mouse was inoculated with 0.1 ml suspension of pretreated A549 cells (1×10^7 cells/mL) into its left armpit. Xenografted mice were divided into three different groups (n = 6 for each group). A549 xenografts were established for 21 days, and tumors were collected.

2.20. Statistical analysis

Each experiment was repeated a minimum of three times. All statistical analyses were performed using SPSS software version 22.0 (IBM SPSS, Inc., Chicago, IL, USA). Statistical significance for most of the data was determined by Student's *t*-test or analysis of variance followed by post hoc tests. Data were presented as mean ± Standard error of the Mean (SEM), and $p < 0.05$ was considered significant.

3. Results

3.1. Klotho is down-regulated in NSCLC samples and associated with survival of NSCLC patients

To verify the association of Klotho and NSCLC, we first measured the endogenous level of Klotho in NSCLC tissues and paracarcinoma tissues obtained from patients using tissue microarray analysis. Among the 69 cases, we observed loss or decreased expression of Klotho in 48 NSCLC tissue samples (69.6%) compared with their corresponding para-carcinoma tissues by immunohistochemistry (IHC) (Fig. 1a). The clinicopathological characteristics of sample cases are summarized according to Klotho expression status in Supplementary Table 1. The results indicate that the protein levels of Klotho in NSCLC tissues are decreased compared with normal lung tissues, while there are no associations identified between clinicopathological characteristics and Klotho expression levels, further large-sample clinical evidence is still needed to support these results. Similar to the IHC results, Klotho protein levels were significantly lower in cancer samples than in normal tissues by western blot (WB) (Fig.1b). Furthermore, we investigated the expression of Klotho in Gene Expression Profiling Interactive Analysis (GEPIA), which is an online tool based on the Cancer Genome Atlas (TCGA) and Genotype-Tissue Expression (GTEx) dataset for transcriptomic analysis, including 969 NSCLC samples and 685 controls. As shown in Fig. 1c, the expression levels of Klotho are significantly lower in lung adenocarcinoma (LUAD) samples ($p < 0.01$) and lung squamous cell carcinoma (LUSC) samples ($p < 0.01$) than control tissues. We also measured the expression of Klotho in several lung cancer cell lines using WB and found particularly low expression in several cell lines, including A549, H1299 and H125 (Fig. 1d). We next explored whether there might exist genomic alterations in Klotho that might correlate with its decreased expression. cBioPortal was used to examine multiple gene alterations, mutations and amplifications of *klotho* in the same NSCLC datasets. In NSCLC, 3% patients had mutations or deletions (Fig. 1e). Interestingly, when browsing the common mutations of *klotho* in NSCLC genomic datasets, we found that *klotho* T968P or its near-neighbor is a mutational hotspot (Fig. 1f).

The effect of Klotho mRNA expression on survival of LUAD and LUSC patients was assessed from Kaplan Meier plotter (www.kmplot.com) using bioinformatic analysis of 1928 cancer samples, of which there were 866 LUAD samples and 675 LUSC samples. The Kaplan-Meier survival curve for the overall lung cancer patients with low or high Klotho expression is shown in Supplementary Fig. S1a. The plots illustrate worse prognosis rates for all patients (HR = 0.72, 95%CI 0.63–0.81, $P = 2.3e\text{-}07$; Supplementary Fig. S1a) and LUAD patients (HR = 0.56, 95%CI 0.44–0.72, $P = 1.9e\text{-}06$) with low Klotho expression, as well as in early stage and never-smokers, while no significant difference is seen in LUSC patients (Supplementary Fig. S1b). The correlations of Klotho expression with different clinical factors were analyzed, including histology, pathological grade, clinical stage, gender and smoking status, and the results are shown in Supplementary Fig. S1b.

3.2. Rab8 interacts with Klotho specifically in NSCLC cells

We next sought to identify Klotho-interacting proteins that may be involved in sub cellular location or trafficking control of Klotho in lung cancer cells. Total protein extracts from A549 cells, which were infected with lentiviral vectors containing FLAG-tagged Klotho (FLAG-KL) were immunoprecipitated (IP) with anti-FLAG antibody. FLAG-GFP constructs were used as negative control to filter out irrelevant background proteins. In order to determine the identity of co-immunoprecipitated proteins, three independent FLAG-KL- and FLAG-GFP- co-immunoprecipitated products were submitted for MS analysis. A total of 77 proteins were identified to coimmunoprecipitate with FLAG-KL. Of these, 37 were assessed as high probability Klotho-binding partners, including 20 members of the Rab family (one of most studied family involved in protein trafficking) exhibiting protein scores over 60 (Fig. 2a, b), and Rab8 achieving the highest overall protein score (The protein score is the sum of the highest ions score for each distinct sequence. This protein score provides a logical order to the report. If multiple queries match to a single protein, but the individual ions scores are below threshold, the combined ions scores can still place the protein high in the report). To further confirm this result, HEK 293 cells were transiently transfected with FLAG-KL and HA-tagged Rab8 (HA-Rab8), and the association between HA-Rab8 and FLAG-KL was then assessed by co-immunoprecipitation. We discovered that Rab8 is bound with Klotho in this ectopic expression setting (Fig. 2c, d). Moreover, we detected endogenous interaction between Rab8 and Klotho under physiological conditions. Rab8/Klotho co-immunoprecipitation assays from whole cell lysates of A549 showed Klotho to be bound with the Rab8 protein even at endogenous levels (Fig. 2e, f). Subsequently, we constructed plasmids containing constitutively active or dominant negative forms of Rab8 to determine the role GTPase activity plays in protein association. Our co-immunoprecipitation experiments showed that the dominant negative form of Rab8 (GDP-binding mutant, Rab8T22N) was bound more tightly with Klotho in comparison with the constitutively active form of Rab8 (GTP-binding mutant, Rab8Q67L) (Fig. 2g). Furthermore, we detected the subcellular co-localization of Klotho with Rab8 in A549 cells by immunocytochemistry. We found that a subset of the Klotho is co-localized with Rab8-containing vesicles in A549 cells (Fig. 2h). Further, we detected the subcellular location KL and Rab8 in different fractionation of cells. As shown in Fig.2i, KL and Rab8 were found mainly in the ER fraction and Golgi apparatus.

These results suggest that Klotho interacts with Rab8, and Rab8 may likewise play a role in Klotho regulation. Similarly, we investigated the expression of Rab8 in GEPIA. As shown in Fig. 2j, the expression level of Rab8 is slightly lower in LUAD and LUSC samples. Measurement of Rab8 expression, with WB in various human lung cancer cell lines revealed that Rab8 expression is lower than in normal lung tissue in some cell lines including A549 and H1299 (Fig. 2k), similar to the results seen in Fig. 1d. Collectively, these results suggest the possibility that the expression level of Rab8 might affect the function of Klotho in NSCLC.

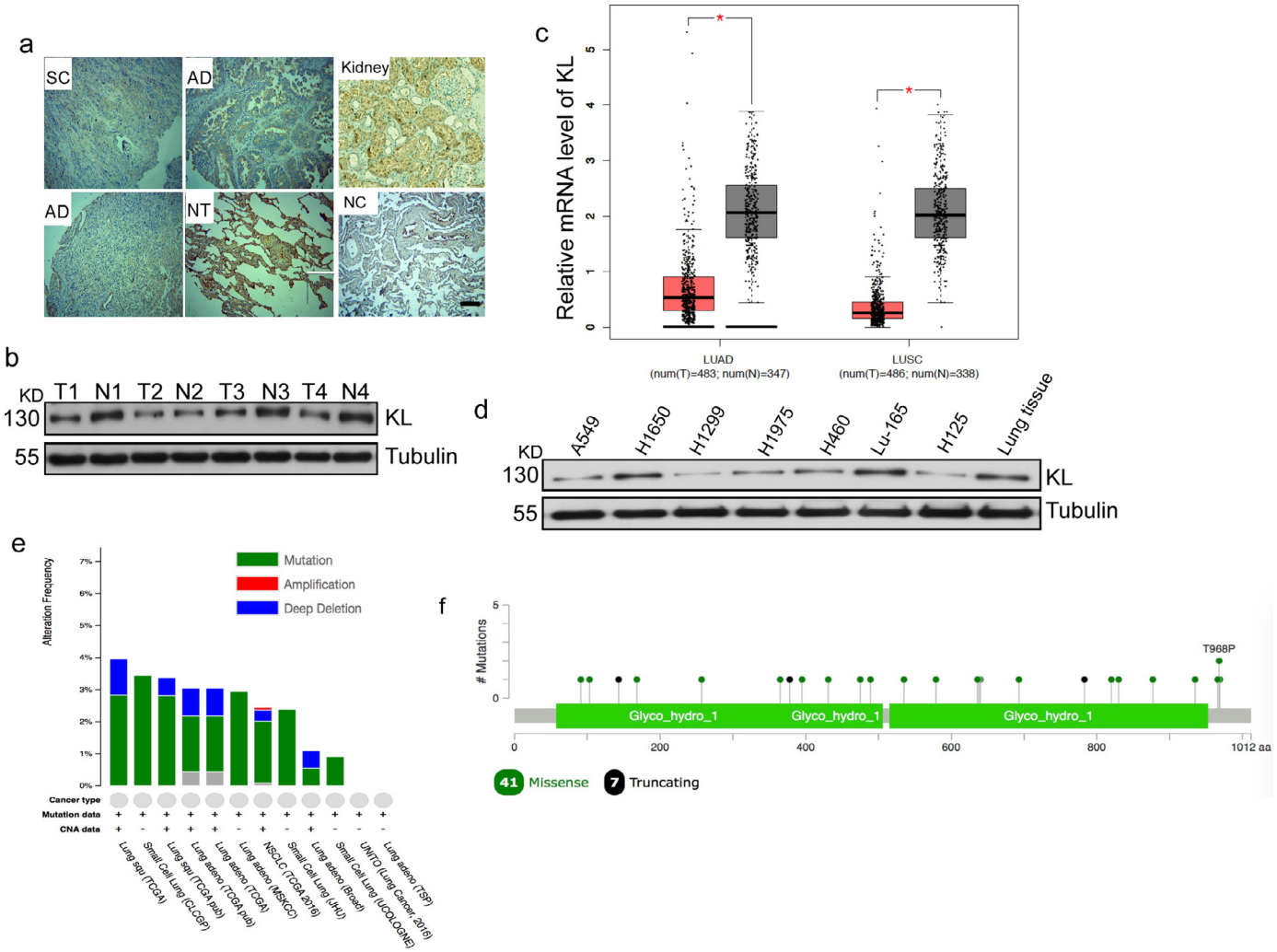

Fig. 1. Klotho is downregulated in NSCLC samples. (a) Klotho (KL) expression was examined by immunohistochemical staining of NSCLC patient tissue microarrays. SC, negative KL expression in lung squamous cell carcinoma (LUSC). AD, negative KL expression in lung adenocarcinoma (LUAD). NT, positive KL expression in normal lung tissue. Kidney tissue as positive control; NC, negative control, no positive staining when omitting primary antibody. (b) Protein expression of KL in NSCLC samples, as measured by WB, relative to that of β-actin. T, tumor. N, normal. Scale bars represent 100 μm. (c) The boxplot of the mRNA expression levels of KL in LUAD and LUSC samples respectively. The y-axis indicated the log2-transformed gene expression level. $^{*}p < 0.05$; Red, cancer samples; gray, normal tissues. (d) Protein expression of KL in different lung cancer cell lines. (e) cBioPortal analysis for genetic alterations of KL (mutations, amplifications and deletions) in lung cancer. (f) Missense alterations in KL. Amino acid substitutions occurring three times are labeled. (For interpretation of the references to color in this figure legend, the reader is referred to the web version of this article.)

3.3. Rab8 regulates surface expression of Klotho in NSCLC cells

To explore the role of Rab8 in Klotho expression, protein and mRNA levels of Klotho were examined via WB and real-time quantitative reverse transcription PCR (qRT-PCR), respectively. We first constructed several small interfering RNAs (siRNAs) targeting Rab8 (siRab8) to knock down endogenous Rab8 (Fig. 3a). As shown, the #1 and #3 Rab8 siRNA transfection reduced about 85% and 91% endogenous Rab8 protein, respectively, as detected by western blot analyses ($n = 3$, $^{*}p < 0.05$, Student's t-test, Fig. 3a). Thus, we mainly used siRab8-3 to explore knockdown effects of Rab8 in this study (thus henceforth siRab8 is used to refer to siRab8-3). We further explored the transcript and protein levels of Klotho in lung cancer cells treated with siRab8-1, siRab8-3or myc-Rab8 plasmids. The results of this treatment show that Rab8 expression does not affect the expression level of Klotho at the mRNA or protein level (Fig. 3b, c).

As Rab8 has also been observed to mediate receptor trafficking, we hypothesized that Rab8 might regulate the cell surface level of Klotho. To explore this hypothesis we performed surface biotinylation assays in the NSCLC cell lines A549 and H1299. We used loss-of-function analyses (Rab8T22N and siRab8) and gain of function analysis (Rab8Q67L) to investigate the role of Rab8 on cell surface expression of Klotho (Fig. 3d, e). As shown, overexpression of Rab8Q67L significantly increased cell surface levels of Klotho in both A549 and H1299 cells (Fig. 3d, e). It is confusing that, Rab8T22N mutant seemed to interact with Klotho better compared with Rab8Q67L active mutant (Fig.2g). However, Rab8T22N showed no or little ability to mediate Klotho presentation on cell surface in Fig 3d, e, f. Similar results have been shown in several research results on Rab11, including our previous study [30, 31]. GDP-blocking Rab11 has a higher affinity with cargo protein, but it exhibits a suppressive function. We suspect that the TN or SN form of Rab protein could bind to cargo protein, but they cannot be converted to GTP-binding membrane-bound form, which limits the transport of cargo protein. Thus, Rab8 may have the same mechanism as Rab11. Conversely, both Rab8T22N and siRab8 significantly reduced the surface levels of Klotho (Fig. 3d, e). It is well known that Klotho can shed from the membrane by metalloproteases like ADAM10 and 17 [32, 33]. If Rab8 reduces ADAM 10/17

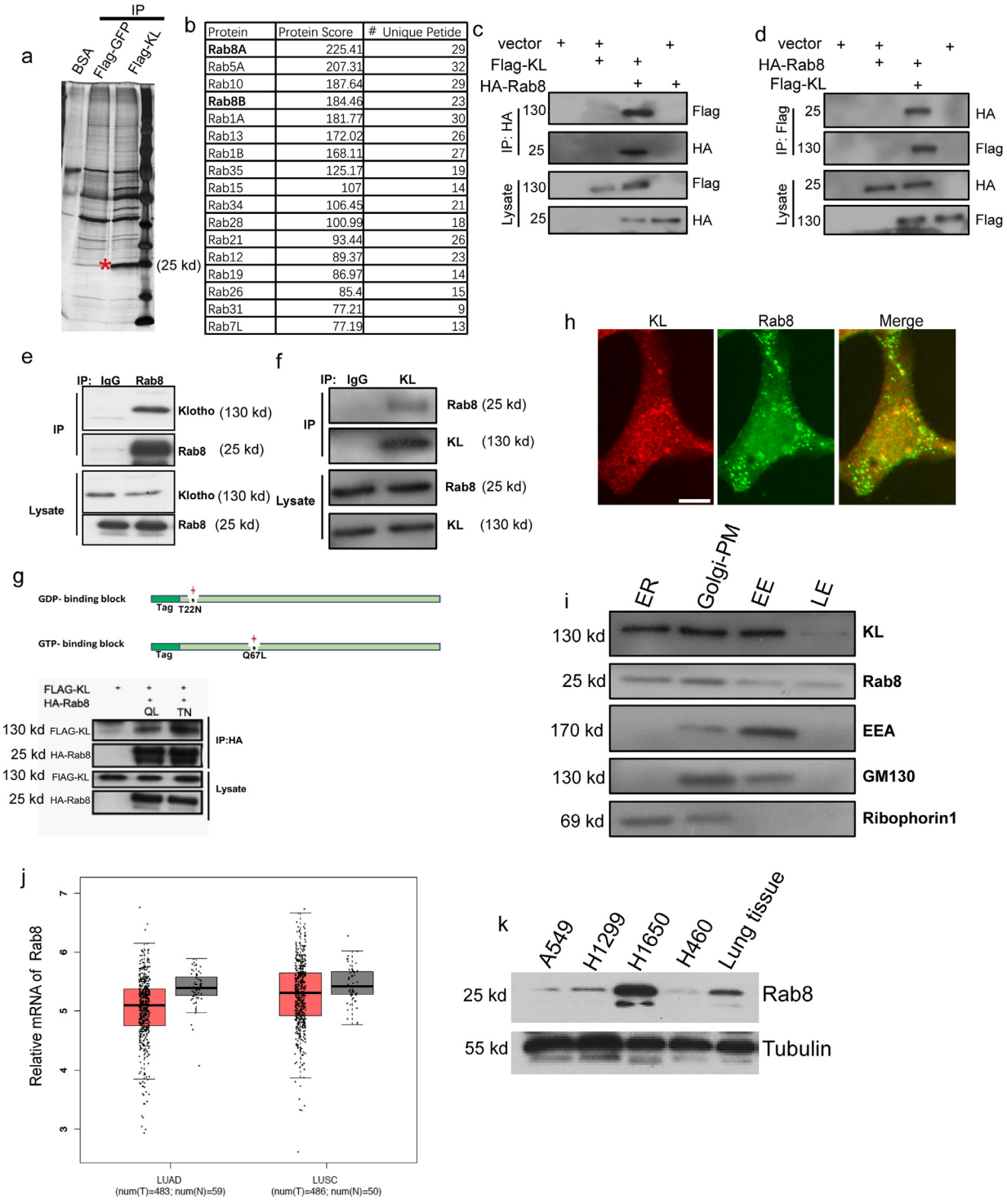

Protein	Protein Score	# Unique Petide
Rab8A	225.41	29
Rab5A	207.31	32
Rab10	187.64	29
Rab8B	184.46	23
Rab1A	181.77	30
Rab13	172.02	26
Rab1B	168.11	27
Rab35	125.17	19
Rab15	107	14
Rab34	106.45	21
Rab28	100.99	18
Rab21	93.44	26
Rab12	89.37	23
Rab19	86.97	14
Rab26	85.4	15
Rab31	77.21	9
Rab7L	77.19	13

Fig. 2. Klotho interacts with Rab8. (a) Silver stain of KL-interacting proteins. FLAG-M2 IP was performed on the cellular extract derived from A549 cells transfected with Flag-GFP (lane 1) or Flag-KL (lanes 2), the red asterisk indicates the bands of possible Rab proteins. (b) A list of Rab proteins pulled down by KL antibodies analyzed by mass spectrometry (MS). (c, d) A549 cells were co-transfected with HA-Rab8 and FLAG-KL constructs, and lysed by RIPA buffer, followed by immunoprecipitation with anti-HA antibody. Western blotting analysis was performed. (e,f) Endogenous association of Rab8 and Klotho in A549 cells was detected by co-immunoprecipitation. (g) A549 cells were co-transfected with HA-Rab8 mutants and FLAG-KL constructs, and lysed by RIPA buffer, followed by immunoprecipitation with anti-HA antibody. Western blotting analysis was performed. (h) Immunocytochemistry staining was carried out with rabbit polyclonal antibody against Klotho (red) and mouse polyclonal antibody against Rab8 (green) in A549 cells. Co-localization of both proteins is shown as merge (yellow). (i) Subcellular localization of Kl and Rab8, Lysates of A549 cells were separated into ER, Golgi-PM, EE, and late endosome (LE) fractions on sucrose gradients, and proteins were blotted either with antibody to Kl, Rab8, early endosome antigen 1 (EEA1), Golgi matrix 130 (GM130), and ribophorin1 antibodies. (j) The boxplot of the mRNA expression of Rab8 in LUAD and LUSC samples. The y-axis indicated the log2-transformed gene expression level. Red, cancer samples; gray, normal tissues. (k) Protein expression of Rab8 in different lung cancer cell lines. (For interpretation of the references to color in this figure legend, the reader is referred to the web version of this article.)

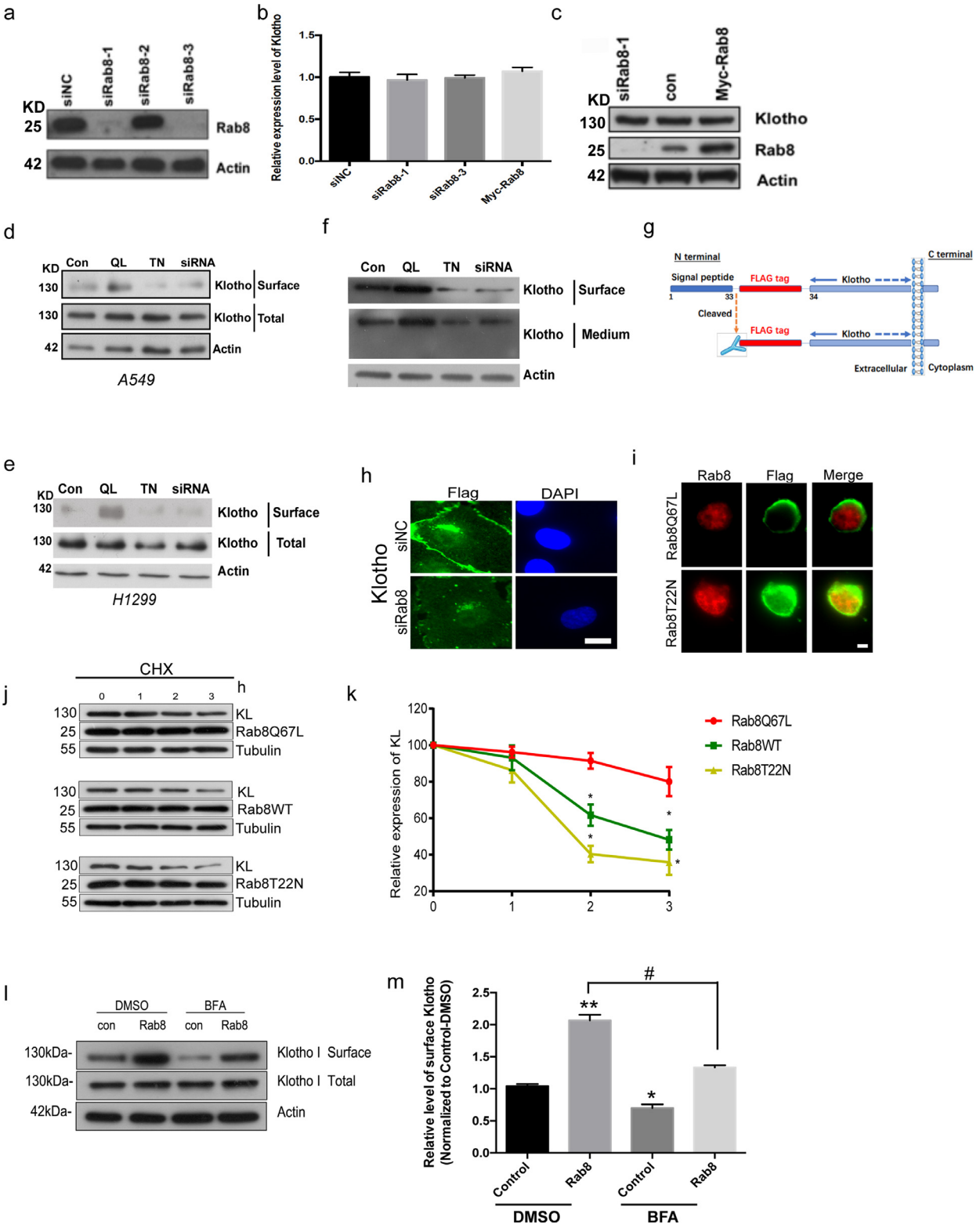

Fig. 3. Rab8 regulates surface expression of Klotho. (a) A549 cells were transfected with Rab8 siRNAs, followed by western blotting assays to detect knockdown efficiency of siRNAs. (b) A549 cells were transfected with siRab8or myc-Rab8, and relative mRNA levels of Klotho were detected by realtime PCR. (c) A549 cells were transfected with siRab8or myc-Rab8, and relative protein levels of Klotho were detected by western blotting assay. (d) A549 cells transfected with Rab8 mutants or siRNA, then followed by surface biotinylation assay. Data shown are the mean ± SEM of three separate experiments (* $p < 0.05$, compared with control group, student's *t*- tests). (e) H1299 cells transfected with Rab8 mutants or siRNA, then followed by surface biotinylation assay. (f) Ra8 mutants or siRNA- transfected A549 cells were incubated in serum-free DMEM for 48 h. The proteins in the medium and surface were analyzed by western blot. ubulin were used as loading controls. (g) FLAG-KL construct with a FLAG epitope after the signal peptide at the C-terminal of full-length Klotho. (h) Representative immunofluorescence images of surface Klotho in A549 cells transfected with siRab8. (i) Representative immunofluorescence images of surface Klotho in A549 cells transfected with Rab8 mutants. (j) A549 cells were transfected with different forms of Rab8 for 48 h and then serum starved for the indicated times at 37 °C in the presence of cycloheximide (CHX, 20μg/ml). Klotho was detected by anti-KL immunoblotting. (k) Data shown are the mean ± SEM of three separate experiments (* $p < 0.05$, analysis of variance followed by post hoc tests). (l) A549 cells transfected with Rab8 and treated with BFA for 4 h, then followed by surface biotinylation assay. (m) Data shown are the mean ± SEM of three separate experiments (* $p < 0.05$, ** $p < 0.01$, # $p < 0.05$, analysis of variance followed by post hoc tests).

expression or affects their sublocalization, the amount of shedded Klotho will decrease, and this may increase Klotho's membrane localization. In order to address this question, we detected the medium Klotho (shedded from membrane) upon Rab8 overexpression or knocking down according to previous report [33]. No detectable changes on the ratio of medium Klotho and surface Klotho were found (Fig. 3f). Also, we investigated whether Rab8 would affect ADAM10/17 expression. As shown in Fig.S2, we found Rab8 does not modulate the expression of ADAM10/17. Thus, we believe that Rab8 does not affect the shedding of Klotho. To detect surface Klotho specifically, we constructed a FLAG-KL construct that contained a FLAG epitope just after the signal peptide (extracellular) of Klotho (Fig. 3g), and subsequently transfected FLAG-KL into lung cancer cells. Surface Klotho was measured by staining with anti-FLAG antibody by immunocytochemistry, under non-permeabilized conditions (antibody can bind with all the epitope outside cell surface under this condition). The results reveal that knockdown of Rab8 by siRNA significantly reduces cell surface levels of Klotho (Fig. 3h). Under permeabilized conditions (antibody can bind with all the epitope outside and inside cell surface under this condition), there are more Klotho co-localized with Rab8T22N compared with Rab8Q67L (Fig. 3i). We also explored whether the location of Klotho could change its degradation kinetics in A549 cells. We measured the degradation of Klotho after blocking its biosynthesis by cycloheximide (CHX), a translation inhibitor. As shown in Fig. 3j and 3k, we found that Rab8Q67L overexpression could significantly decrease Klotho degradation in A549 cells, while Rab8T22N increase the Klotho degradation.

Overall, our results indicate that Rab8 might indirectly regulate Klotho degradation by modulating translocation of Klotho onto the cell surface. Indeed, previous studies have indicated that Rab8 is localized to the Golgi region, and can serve as a regulator of post-Golgi membrane traffic from the TGN to the plasma membrane [27]. To examine whether Rab8 regulates the traffic of KL from TGN to cell surface, we treated the cells co-expressing Flag-KL and Rab8 with Brefeldin A (BFA), which is a lactone antibiotic that disassembles the Golgi apparatus and blocks anterograde transport of membrane proteins from the ER to the Golgi apparatus. When treated with BFA, Rab8 failed to affect the surface expression of KL (Fig. 3l, 3m), suggesting that Rab8 regulates the biosynthetic trafficking pathways of KL from the TGN to the cell surface. Further, we performed immunocytochemistry assay to confirm it. As shown in Fig. S3, we found Rab8 TN mutants could trap KL in Golgi.

3.4. Rab8 modulates surface levels of Klotho via the post-biosynthetic pathway, but not the endocytic pathway

The surface level of proteins depends on the balance between insertion and endocytosis, two opposing receptor trafficking processes. We designed an experiment to determine which of the two processes affecting Klotho surface expression might be regulated by Rab8. To that effect, we performed a cleavable surface biotinylation assay to measure Klotho internalization. The results show that 40% ± 5% of surface Klotho was internalized 30 min after biotin labeling, and was not affected by overexpression of Rab8 (Fig. 4a–c). These findings suggest that Rab8 is not involved in Klotho internalization. There are two alternate endocytic fates that Klotho can follow, being degradated or recycling back to the plasma membrane. Recycling of protein back to the plasma membrane can cause functional resensitization. Thus, whether Rab8 could regulate Klotho recycling was determined (Fig. 4d, e). We used a live cell ratiometric fluorescence-based recycling assay based on a previous study[28] to measure Klotho recycling. Quantification of these results by ratiometric analyses (see "Methods") confirmed that Rab8 does not affect recycling level of Klotho (Fig. 4f). We further performed the surface biotinylation assay to detect the recycled Klotho, and the result is shown as Fig. 4g. The "rewarming" group showed decreased protein level compared with "internalized" group, the "disappeared" protein was recycled back to the cell surface and washed out [28]. The result confirms that Rab8 does not affect the recycling of KL also. These results suggest that Rab8 does not affect the endocytosis of Klotho. Therefore, the overall results suggest that Rab8 may modulate surface levels of Klotho via the post-biosynthetic pathway, but not the endocytic pathway.

3.5. Rab8 is involved in the cell function regulation of Klotho in NSCLC cells

We next aimed to further investigate whether Rab8 affects Klotho-related cell functions. We previously reported that Klotho is involved in the proliferation and migration of lung cancer cells [11]. Specifically, overexpression of Klotho was shown to inhibit proliferation and migration ability of A549 cells. We thus first examined whether Rab8 might modulate the effects of Klotho on lung cancer cell proliferation. As shown in Fig. 5a, the results from the CCK8 assay showed that proliferation of A549 and H1299 cells was inhibited by Klotho regardless of Rab8 expression, while Rab8 overexpression could enhance the growth inhibition of A549 and H1299 cells upon Klotho transfection. The results suggest that Rab8 itself does not significantly affect lung cancer cell proliferation, but could increase Klotho function on growth inhibition. Subsequently, we conducted a colony formation assay and got the similar results (Fig. 5b).

We next further explored whether Rab8 is involved in other functions of Klotho, such as cell migration. Toward this end, we performed a wound healing assay, as shown in Fig. 5c and d, and observed that Klotho overexpression markedly inhibits lung cancer cell migration into wound areas in NC group cells. However, in Rab8 overexpression group, the Klotho showed more significant effect on migration inhibition. Meanwhile, we found that Rab8 itself cannot affect lung cancer cell migration (Fig. 5c, d). These results suggest that Rab8 can effectively modulate the function of endogenous Klotho in lung cancer cell migration.

To confirm this result, we also tested cell invasion efficiency using transwell invasion assay. As shown in Fig. 5e and f, lung cancer cells with ectopic expression of Klotho displayed a significant decrease of invasion efficiency in NC group; whereas in the Rab8 overexpression group, Klotho overexpression inhibited the invasiveness ability of lung cancer cells more significantly. Similarly, we found that Rab8 itself can not affect cell invasion of A549 and H1299 cells. Thus, Rab8 can also modulate the function of endogenous Klotho in lung cancer cell invasion. Taken together, our results indicated that Rab8 is a critical molecule for Klotho-mediated cell migration and invasion in NSCLC cells.

3.6. Rab8 is involved in the Klotho-mediated regulation of epithelial-mesenchymal transition (EMT) in NSCLC cells

We also explored whether Rab8 might have an effect on Klotho-modulated EMT in NSCLC cells by performing WB to analyze EMT-related markers in A549 and H1299 cells transfected with siRab8 and/or FLAG-KL (Fig. 6a, b). E-Cadherin was upregulated in both A549 and H1299 cells transfected with FLAG-KL compared to control cells, while co-transfection with siRab8 blocked this response. At the same time, a downregulation of N-Cadherin and Vimentin was also induced by Klotho in both types of cells. siRab8 could also abolish this Klotho-mediated effect in both cell types. These changes in EMT-related biomarkers suggest that Klotho can inhibit the transition of epithelial cells to mesenchymal cells, while siRab8 could impair this function.

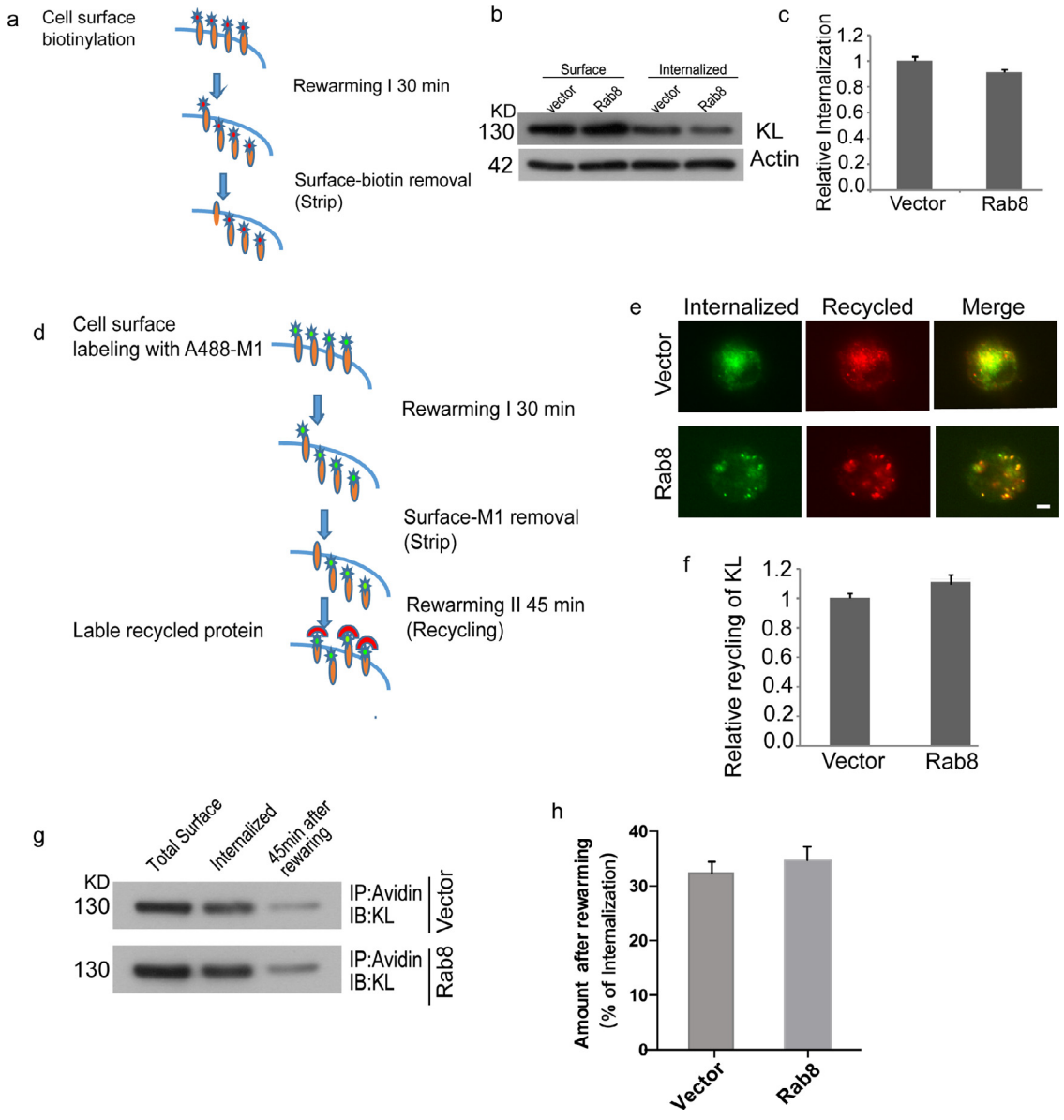

Fig. 4. Rab8 does not affect the internalization and recycling of Klotho. (a) Cartoon showing work steps of cleavable surface biotinylation assay. (b) A549 cells were transfected with Rab8, followed by cleavable surface biotinylation assays to detect the internalization of KL. (c) Relative level of internalization of KL at 30 min after biotin labeling. Data were presented as internalization percentage of total surface KL protein. (d) Cartoon showing work steps of recycling assay. (e) A549 cells expressing FLAG-tagged KL were incubated at 4 °C for 30 min with fluoresceinated (Alexa-488) anti-FLAG antibodies (M1) (2 μg/ml) and then incubated at 37 °C with DMEM for 30 min (rewarming I). A488-M1 (green) was used to label internalized KL. Afterward, the noninternalized anti-FLAG antibodies were stripped with EDTA, and cells incubated in the presence of 10 μg/ml anti-Alexa-594 mouse antibodies for 45 min (rewarming II) to detect the recycled KL (Recycled, red). Representative immunofluorescence images of recycled KL in transiently transfected A549 cells. Total internalized KL are shown in green, the recycled KL is shown in red. (f) Relative recycling levels of KL in A549 cells. Graphs represent means ± SEM of five independent experiments ($n = 30$ cells, for each condition per experiment, Student's t-test). (g) The surface biotinylating assay to detect the recycled KL. Total surface refers to the total biotinylated KL on the cell surface; Internalization refers to the internalized biotinylated receptors before rewarming. (h) No significant change of the recycle fate of KL was detected upon Rab8 overexpression. (For interpretation of the references to color in this figure legend, the reader is referred to the web version of this article.)

3.7. Rab8 is involved in Klotho-mediated regulation of the Wnt signaling pathway in NSCLC cells

We also investigated whether Rab8 might be involved in the function of Klotho in signaling pathway regulation. It has been reported by us and others that Klotho is involved in the regulation of the Wnt signaling pathway, which is associated with cancer development and progression. Thus, we explored whether Rab8 knockdown affects Wnt signaling induced by Klotho overexpression in A549 and H1299 cells. As shown in Fig. 6c and d, in the siNC group, Klotho could reduce the expression levels of active β-catenin and Wnt3a; while in siRab8 group, we found that Rab8 knockdown by siRNA almost abolishes this effect. Additionally, we detected the nuclear location of β-catenin by immunocytochemistry in A549 cells. As shown in Fig. 6e, Klotho overexpression also inhibited the translocation of β-catenin into the nucleus; while in the siRab8 group, this effect of Klotho was abolished. Finally, we detected the expression level of the Wnt signaling pathway target genes c-myc and cyclin D1. We found that in siNC group, Klotho overexpression could inhibit the expression of c-myc and cyclin D1; while in siRab8 group, this effect was also abolished (Fig. 6f). Alternatively, Rab8 knockdown did not affect IGF-1 signaling or p53 levels affected by Klotho overexpression in A549 cells (Supplementary Fig. S4).

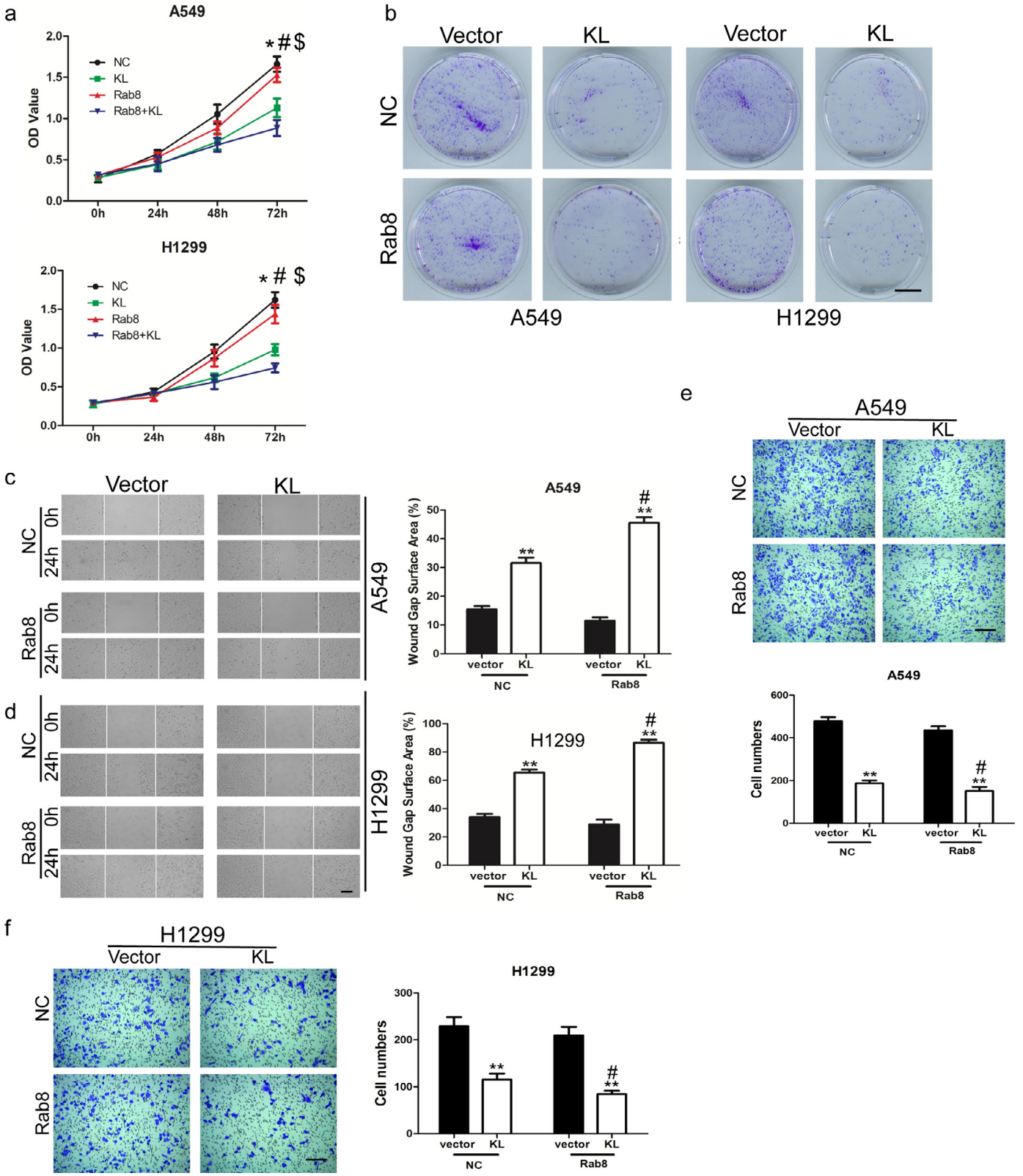

Fig. 5. Rab8 is involved in the cell function regulation of Klotho. (a) After transfection with KL and/or Rab8 plasmid for 48 h, the proliferation of A549 and H1299 cells was measured as indicated times by CCK-8 assay. Values are mean ± SEM; $n = 3$ independent experiments. $^{*}p < 0.05$, compared with 0 h; # $p < 0.05$, KL group *vs* control group; $ $p < 0.05$, KL+Rab8 group *vs* Rab8 group, one-way ANOVA. (b) Colony formation of A549 and H1299 cells was analyzed by crystal violet staining. Scale bars represent 50 μg. (c) Impact of Rab8 and KL on A549 cells migration by wound-healing assay and quantitative analysis of the wound-healing assay. ** $p < 0.01$, compared with NC–Con group; # $p < 0.05$, KL+Rab8 group *vs* Rab8 group one-way ANOVA. Scale bars represent 50 μg. (d) Impact of Rab8 and KL on H1299 cells migration by wound-healing assay and quantitative analysis of the wound-healing assay. ** $p < 0.01$, compared with NC–Con group; # $p < 0.05$, KL+Rab8 group *vs* Rab8 group, one-way ANOVA. (e) Impact of Rab8 and KL on A549 cells invasion by transwell assay. ** $p < 0.01$, compared with NC–Con group; # $p < 0.05$, KL+Rab8 group *vs* Rab8 group, one-way ANOVA. (f) Impact of Rab8 and KL on H1299 cells invasion by transwell assay. Scale bars represent 50 μg. ** $p < 0.01$, compared with NC–Con group; # $p < 0.05$, KL+Rab8 group *vs* Rab8 group one-way ANOVA.

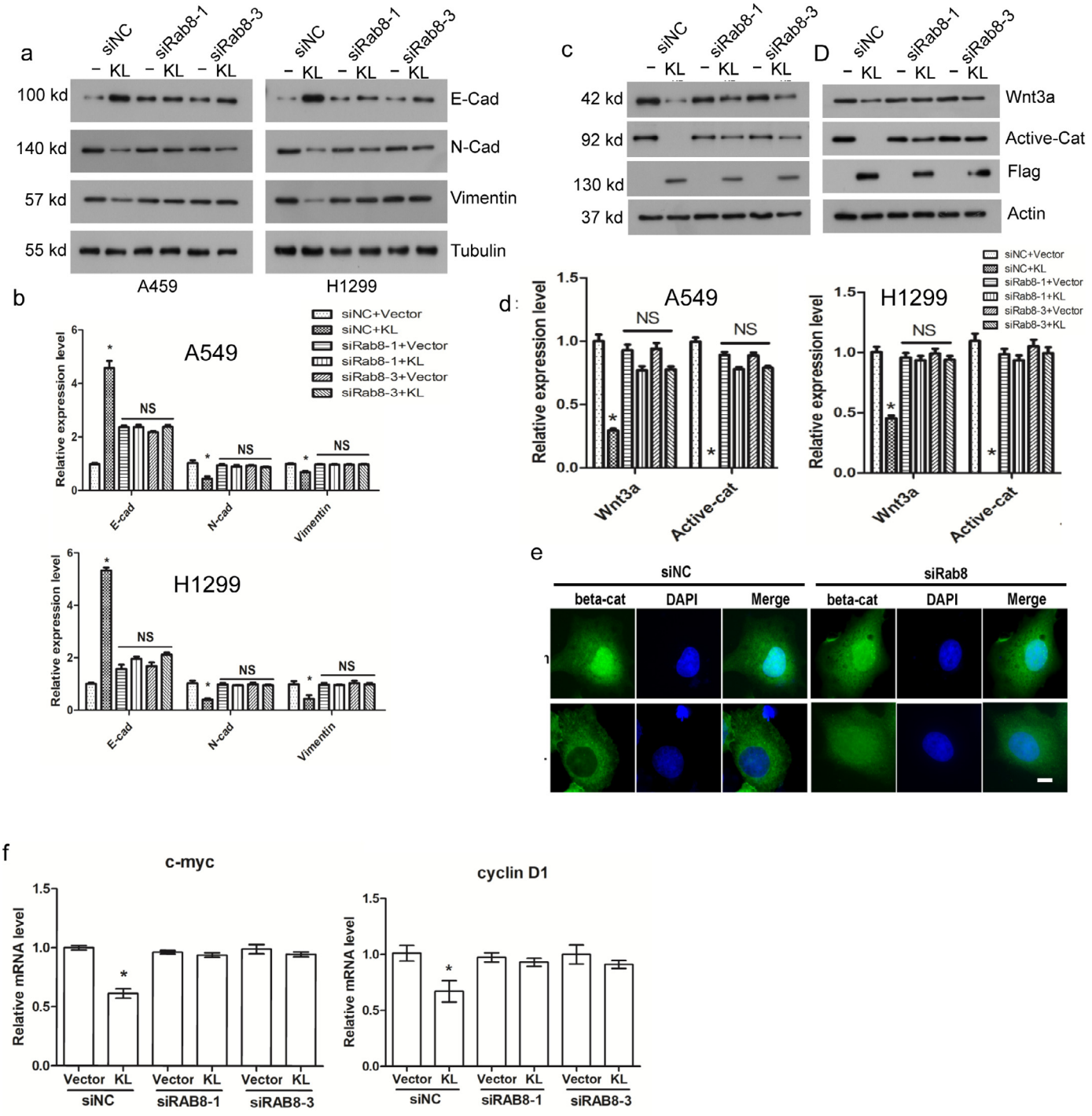

Fig. 6. Rab8 is involved in the Klotho-mediated regulation of EMT markers and Wnt signaling pathway in NSCLC cells. (a) A549 and H1299 cells were transfected with siRab8 and/or KL, followed by western blotting assays to detect expression level of indicated EMT marker proteins. (b) Quantitative analysis of western blotting results as shown in (a). $^{*}p < 0.05$, compared with siNC-vector group; one-way ANOVA. (c) A549 cells were transfected with siRab8 and/or KL, followed by western blotting assays to detect expression level of indicated proteins. $^{*}p < 0.05$, compared with siNC-vector group; one-way ANOVA. (d) H1299 cells were transfected with siRab8 and/or KL, followed by western blotting assays to detect expression level of indicated proteins. $^{*}p < 0.05$, compared with siNC-vector group; one-way ANOVA. (e) Colocalization of endogenous β-catenin with DAPI in A549 cells is revealed by standard fluorescent microscopy. Merged images of β-catenin (green) and DAPI (blue) staining are shown. (f) A549 cells were transfected with siRab8 and/or KL, and relative mRNA levels of cyclin D1 and c-myc were detected by realtime PCR. $^{*}p < 0.05$, compared with siNC-Vector group; one-way ANOVA. (For interpretation of the references to color in this figure legend, the reader is referred to the web version of this article.)

These results strongly suggested that Rab8 is involved in the function of Klotho on Wnt signaling pathway regulation. To verify whether the Wnt signaling pathway is involved in KL-mediated regulation of EMT, we tested whether a sustained-activated form of beta-catenin lacking the NH2-terminal 90 amino acids (Δ N90-beta-catenin) [34] could block KL's regulation of EMT. The results showed that KL is unable to regulate EMT-related proteins in cells overexpressing Δ N90-beta-catenin, thereby suggesting that the Wnt signaling pathway is involved in KL-regulated EMT (Supplementary Fig. S4). Further, we found that Δ N90-beta-catenin could

abolish the KL function on inhibiting invasion of A549 cells Supplementary Fig. S4.

3.8. *Rab8 overexpression increases Klotho-mediated inhibition of NSCLC tumorigenesis* in vivo

To further verify the *in vitro* findings, we monitored the growth of tumors derived from A549 cells infected with KL or KL/Rab8 in a xenograft mouse model. Consistent with our *in vitro* findings, tumors derived from KL/Rab8-co-infected A549 cells grew at a much slower rate than those derived from vector or KL transfected cells, as reflected in significantly smaller tumor sizes (Fig. 7a) and tumor weights (Fig. 7b) at three weeks after cell implantation. In addition, we performed immunohistochemistry to observe the surface expression of Klotho in the xenograft tumor tissue. As shown in Fig. 7c, we found that, with Rab8 overexpression, Klotho was expressed to a greater extent on the surface when compared with KL-infected only group. These results from the mouse xenograft model suggest that Klotho can inhibit NSCLC tumorigenesis *in vivo*, and Rab8 overexpression can amplify the antitumorigenic effects of Klotho.

4. Discussion

Tumor suppressor capabilities of Klotho have now been implicated in numerous physiological activities and signaling pathways beyond those originally discovered by Kuro-o and his colleagues [3, 35]. Given that Klotho is a type-I membrane protein, its functions are expected to be closely related to its sublocation and metabolism kinetics. In the present study, we demonstrated that this is indeed the case by providing evidence that Rab8 is co-localized and associated with Klotho, modulates the surface expression level of Klotho, and is critical for Klotho function in lung cancer. The schematics of the proposed mechanisms are shown in Fig. 7d.

Rab proteins belong to the monomeric GTPases of the Ras superfamily. Rabs are localized on the cytoplasmic surface of specific intracellular compartments and vesicles, and are involved in the control of vesicular trafficking [36]. Functional impairments of Rab proteins have been implicated in tumorigenesis, including Rab1, Rab2A, Rab3 D, Rab8 and others [37–39]. Rab8 is a small Ras-related GTPase, involved in protein trafficking and secretion [27]. In humans there are two isoforms with 80% homology, Rab8a and Rab8b. They have a differential expression pattern. Rab8b is expressed mainly in the spleen, testis and brain. Rab8a, on the other hand, is more ubiquitously expressed but shows only limited expression levels in these three organs [40]. Likewise Rab8a is expected to be the main isoform present in human lung tissues and associated cancers. Rab8a and Rab8b have also both been shown to play a similar role in vesicular traffic [39, 40]. Rab8 has been reported to transport many critical proteins, such as AMPAR and TfR. Rab8 mainly regulates trafficking of protein from the trans-Golgi network (TGN) to the cell surface, an important process in cell biology [27]. Rab8 has also been found to enhance TMEM205-mediated cisplatin resistance in human epidermoid carcinoma cell line KB-3-1 [41]. It has been reported that Rab8 transports exocytic vesicles transporting membrane type 1-matrix metalloproteinase (MT1-MMP) to the plasma membrane for matrix degradation of migrating cancer cells [42]. Hattula and colleagues reported that Rab8 can be localized to recycling vesicles that fuse with the plasma membrane, thereby making the membranes suitable for protrusion formation [43].

In this study, we report for the first time that Rab8 is co-localized and associated with Klotho, and Klotho trafficking is regulated by Rab8, furthers extending our understanding of Klotho. Klotho is known to be a regulator of protein transport across the cell membrane by directly affecting transporter proteins [44]. However, little is known about trafficking control of the Klotho protein itself. The present works demonstrates that Rab8 interacts with Klotho, and regulates the surface level of Klotho without affecting its total protein level in NSCLC cells. That is to say, Rab8 regulates the traffic of Klotho in lung cancer cells. It is widely known that the surface level of proteins depends on the balance between insertion and endocytosis, two opposing receptor trafficking processes. There are two alternate endocytic fates that Klotho can follow, being delivered to lysosomes for degradation, or recycled back to the plasma membrane. Recycling of protein back to the plasma membrane can cause functional resensitization [45]. Our results showed that Rab8 is not involved in Klotho internalization, and confirmed that Rab8 does not affect recycling of Klotho. Additionally, our results also showed that, when treated with BFA, Rab8 failed to affect the surface expression of Klotho, while Rab8 TN mutants could trap KL in Golgi. All the results suggest that Rab8 regulates the biosynthetic trafficking pathways of KL from the TGN to the cell surface.

Our study and others have previously shown that Klotho inhibits cancer cell growth and motility by regulating the Wnt signaling pathway [11, 18, 20, 23–25]. Wnt activation causes synthesis of its target genes that may promote cancer cell growth or motility and contribute to the induction of EMT via stimulating several EMT-related transcription factors [46]. In this work, we report that Rab8 is involved in Klotho-mediated regulation of Wnt-β-catenin signaling, EMT marker expression, cell proliferation, migration and invasiveness in NSCLC cells. Our results show that Rab8 can regulate Klotho-mediated inhibition of the Wnt signaling activity by modulating translocation of Klotho to the cell surface, which in turn affects Klotho-mediated function in NSCLC. Klotho expression has also been shown to correlate with a number of factors associated with EMT in cervical cancers [16] and lung cancers [9]. Similarly, our results provide new clues on the Klotho-mediated EMT regulation of NSCLCs cells, which is under control of Rab8.

Overall, our results provide new insight into the mechanism underlying Klotho functions in NSCLC. First of all, we found that Rab8 is a regulator of Klotho surface expression. In particular, our results reveal that the surface expression level of Klotho is highly influenced by Rab8, and that Rab8 regulates Klotho-dependent Wnt signaling and function in NSCLC cells. Furthermore, our study provides a working model for Rab8 function in the context of cancer and cancer biology.

Declarations of Competing Interest

The authors declare that they have no competing interests.

CRediT authorship contribution statement

Bo Chen: Data curation, Formal analysis, Funding acquisition, Investigation, Project administration, Writing - original draft. **Shuhong Huang:** Data curation, Formal analysis, Funding acquisition, Investigation, Project administration, Writing - original draft. **Thomas R. Pisanic, II:** Investigation, Writing - original draft. **Alejandro Stark:** Investigation, Writing - original draft. **Yong Tao:** Investigation, Writing - original draft. **Bei Cheng:** Investigation, Writing - original draft. **Yue Li:** Investigation. **Yunyan Wei:** Investigation. **Jianqing Wu:** Funding acquisition, Project administration, Writing - review & editing.

Acknowledgments

This study was supported by the International Science & Technology Cooperation Program of China (No. 2014DFA31940); The National Natural Science Foundation of China (Nos. 81572259,

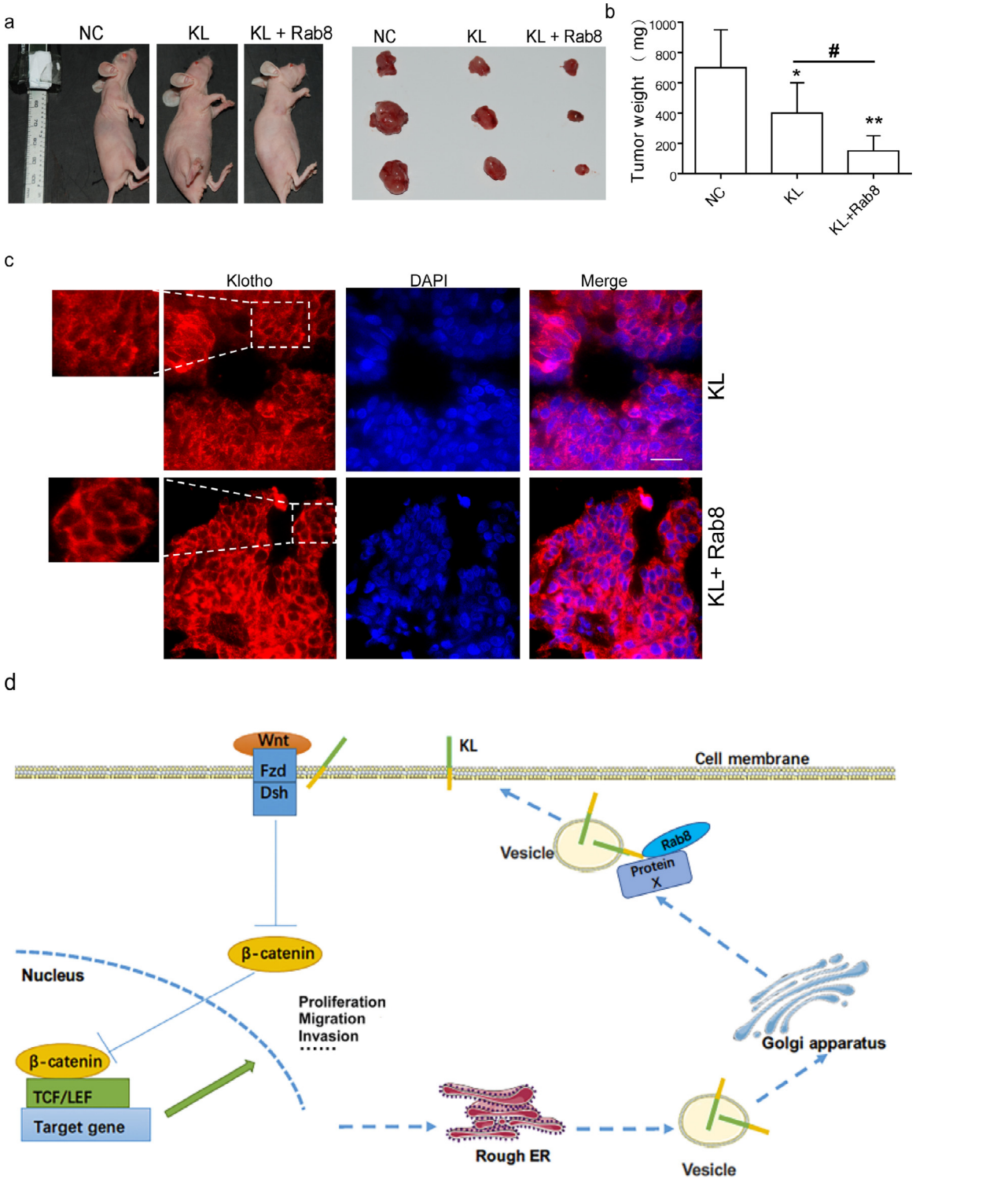

Fig. 7. Rab8 overexpression increases the function of Klotho on inhibiting NSCLC tumorigenesis *in vivo*. (a) The nude mice were inoculated with either A549 cells stablly expressing KL or KL/Rab8, and the xenograft tumors were photographed. (b) Tumor volume and weight at the end point (3 weeks). * $p < 0.05$, ** $p < 0.01$, compared with NC group; # $p < 0.05$, KL *vs* KL+Rab8; one-way ANOVA. (c) Klotho (KL) expression was examined by immunohistochemical staining of tumor xenograft. Scale bars represent 50 μg. (d) Schematics of proposed relationship of KL, Rab8 and Wnt signaling pathway.

81302011 and 81971088); The Jiangsu Province's Youth Medical Talents Program (No. QNRC2016593); The Jiangsu Provincial Key Discipline of Medicine (No. ZDXKA2016003); The Six Talent Peaks Project in Jiangsu Province (No. 2018-WSN-003). The funders had no role in the study design, data collection, data analysis, interpretation, or writing of the paper.

Supplementary materials

Supplementary material associated with this article can be found, in the online version, at doi:10.1016/j.ebiom.2019.10.040.

References

[1] Siegel RL, Miller KD, Jemal A. Cancer statistics, 2018. CA Cancer J Clin 2018;68:7–30.
[2] Goldstraw P, Ball D, Jett JR, Le Chevalier T, Lim E, Nicholson AG, Shepherd FA. Non-small-cell lung cancer. Lancet 2011;378:1727–40.
[3] Kuro-o M, Matsumura Y, Aizawa H, Kawaguchi H, Suga T, Utsugi T, Ohyama Y, Kurabayashi M, Kaname T, Kume E, et al. Mutation of the mouse klotho gene leads to a syndrome resembling ageing. Nature 1997;390:45–51.
[4] Kurosu H, Yamamoto M, Clark JD, Pastor JV, Nandi A, Gurnani P, McGuinness OP, Chikuda H, Yamaguchi M, Kawaguchi H, et al. Suppression of aging in mice by the hormone Klotho. Science 2005;309:1829–33.
[5] Xu Y, Sun Z. Molecular basis of Klotho: from gene to function in aging. Endocr Rev 2015;36:174–93.
[6] Sato S, Kawamata Y, Takahashi A, Imai Y, Hanyu A, Okuma A, Takasugi M, Yamakoshi K, Sorimachi H, Kanda H, et al. Ablation of the p16(INK4a) tumour suppressor reverses ageing phenotypes of klotho mice. Nat Commun 2015;6:7035.
[7] Ligumsky H, Rubinek T, Merenbakh-Lamin K, Yeheskel A, Sertchook R, Shahmoon S, Aviel-Ronen S, Wolf I. Tumor suppressor activity of Klotho in breast cancer is revealed by structure-function analysis. Mol Cancer Res 2015;13:1398–407.
[8] Wolf I, Levanon-Cohen S, Bose S, Ligumsky H, Sredni B, Kanety H, Kuro-o M, Karlan B, Kaufman B, Koeffler HP, Rubinek T. Klotho: a tumor suppressor and a modulator of the IGF-1 and FGF pathways in human breast cancer. Oncogene 2008;27:7094–105.
[9] Ibi T, Usuda J, Inoue T, Sato A, Takegahara K. Klotho expression is correlated to molecules associated with epithelial-mesenchymal transition in lung squamous cell carcinoma. Oncol Lett 2017;14:5526–32.
[10] Wang Y, Chen L, Huang G, He D, He J, Xu W, Zou C, Zong F, Li Y, Chen B, et al. Klotho sensitizes human lung cancer cell line to cisplatin via PI3k/Akt pathway. PLoS ONE 2013;8:e57391.
[11] Chen B, Ma X, Liu S, Zhao W, Wu J. Inhibition of lung cancer cells growth, motility and induction of apoptosis by Klotho, a novel secreted Wnt antagonist, in a dose-dependent manner. Cancer Biol Ther 2012;13:1221–8.
[12] Usuda J, Ichinose S, Ishizumi T, Ohtani K, Inoue T, Saji H, Kakihana M, Kajiwara N, Uchida O, Nomura M, et al. Klotho is a novel biomarker for good survival in resected large cell neuroendocrine carcinoma of the lung. Lung Cancer 2011;72:355–9.
[13] Chen B, Wang X, Zhao W, Wu J. Klotho inhibits growth and promotes apoptosis in human lung cancer cell line A549. J Exp Clin Cancer Res 2010;29:99.
[14] Abramovitz L, Rubinek T, Ligumsky H, Bose S, Barshack I, Avivi C, Kaufman B, Wolf I. KL1 internal repeat mediates klotho tumor suppressor activities and inhibits bFGF and IGF-I signaling in pancreatic cancer. Clin Cancer Res 2011;17:4254–66.
[15] Lojkin I, Rubinek T, Orsulic S, Schwarzmann O, Karlan BY, Bose S, Wolf I. Reduced expression and growth inhibitory activity of the aging suppressor klotho in epithelial ovarian cancer. Cancer Lett 2015;362:149–57.
[16] Chang B, Kim J, Jeong D, Jeong Y, Jeon S, Jung SI, Yang Y, Kim KI, Lim JS, Kim C, Lee MS. Klotho inhibits the capacity of cell migration and invasion in cervical cancer. Oncol Rep 2012;28:1022–8.
[17] Li XX, Huang LY, Peng JJ, Liang L, Shi DB, Zheng HT, Cai SJ. Klotho suppresses growth and invasion of colon cancer cells through inhibition of IGF1 R-mediated PI3K/AKT pathway. Int J Oncol 2014;45:611–18.
[18] Tang X, Wang Y, Fan Z, Ji G, Wang M, Lin J, Huang S, Meltzer SJ. Klotho: a tumor suppressor and modulator of the Wnt/beta-catenin pathway in human hepatocellular carcinoma. Lab Invest 2016;96:197–205.
[19] Zhu Y, Xu L, Zhang J, Xu W, Liu Y, Yin H, Lv T, An H, Liu L, He H, et al. Klotho suppresses tumor progression via inhibiting PI3K/Akt/GSK3beta/Snail signaling in renal cell carcinoma. Cancer Sci 2013;104:663–71.
[20] Camilli TC, Xu M, O'Connell MP, Chien B, Frank BP, Subaran S, Indig FE, Morin PJ, Hewitt SM, Weeraratna AT. Loss of Klotho during melanoma progression leads to increased filamin cleavage, increased Wnt5A expression, and enhanced melanoma cell motility. Pigment Cell Melanoma Res 2011;24:175–86.
[21] Kasprzak A, Kwasniewski W, Adamek A, Gozdzicka-Jozefiak A. Insulin–like growth factor (IGF) axis in cancerogenesis. Mutat Res Rev Mutat Res 2017;772:78–104.
[22] Krishnamurthy N, Kurzrock R. Targeting the Wnt/beta-catenin pathway in cancer: update on effectors and inhibitors. Cancer Treat Rev 2018;62:50–60.
[23] Lee J, Jeong DJ, Kim J, Lee S, Park JH, Chang B, Jung SI, Yi L, Han Y, Yang Y, et al. The anti-aging gene Klotho is a novel target for epigenetic silencing in human cervical carcinoma. Mol Cancer 2010;9:109.
[24] Sun H, Gao Y, Lu K, Zhao G, Li X, Li Z, Chang H. Overexpression of Klotho suppresses liver cancer progression and induces cell apoptosis by negatively regulating wnt/beta-catenin signaling pathway. World J Surg Oncol 2015;13:307.
[25] Tang X, Fan Z, Wang Y, Ji G, Wang M, Lin J, Huang S. Expression of klotho and beta-catenin in esophageal squamous cell carcinoma, and their clinicopathological and prognostic significance. Dis Esophagus 2016;29:207–14.
[26] Urakawa I, Yamazaki Y, Shimada T, Iijima K, Hasegawa H, Okawa K, Fujita T, Fukumoto S, Yamashita T. Klotho converts canonical FGF receptor into a specific receptor for FGF23. Nature 2006;444:770–4.
[27] Peranen J. Rab8 GTPase as a regulator of cell shape. Cytoskeleton (Hoboken) 2011;68:527–39.
[28] Huang SH, Zhao L, Sun ZP, Li XZ, Geng Z, Zhang KD, Chao MV, Chen ZY. Essential role of Hrs in endocytic recycling of full-length TrkB receptor but not its isoform trkb.t1. J Biol Chem 2009;284:15126–36.
[29] Delcroix JD, Valletta JS, Wu C, Hunt SJ, Kowal AS, Mobley WC. NGF signaling in sensory neurons: evidence that early endosomes carry NGF retrograde signals. Neuron 2003;39:69–84.
[30] Huang SH, Wang J, Sui WH, Chen B, Zhang XY, Yan J, Geng Z, Chen ZY. BDNF-dependent recycling facilitates TrkB translocation to postsynaptic density during LTP via a Rab11-dependent pathway. J Neurosci 2013;33:9214–30.
[31] Parent A, Hamelin E, Germain P, Parent JL. Rab11 regulates the recycling of the beta2-adrenergic receptor through a direct interaction. Biochem J 2009;418:163–72.
[32] Bloch L, Sineshchekova O, Reichenbach D, Reiss K, Saftig P, Kuro-o M, Kaether C. Klotho is a substrate for alpha-, beta- and gamma-secretase. FEBS Lett 2009;583:3221–4.
[33] Chen CD, Podvin S, Gillespie E, Leeman SE, Abraham CR. Insulin stimulates the cleavage and release of the extracellular domain of Klotho by ADAM10 and ADAM17. Proc Natl Acad Sci U S A 2007;104:19796–801.
[34] Imbert A, Eelkema R, Jordan S, Feiner H, Cowin P. Delta N89 beta-catenin induces precocious development, differentiation, and neoplasia in mammary gland. J Cell Biol 2001;153:555–68.
[35] Rubinek T, Wolf I. The role of Alpha-Klotho as a universal tumor suppressor. Vitam Horm 2016;101:197–214.
[36] Cheng KW, Lahad JP, Gray JW, Mills GB. Emerging role of RAB GTPases in cancer and human disease. Cancer Res 2005;65:2516–19.
[37] Guadagno NA, Progida C. Rab GTPases: switching to human diseases. Cells 2019;8.
[38] Banworth MJ, Li G. Consequences of RAB GTPase dysfunction in genetic or acquired human diseases. Small GTPases 2018;9:158–81.
[39] Tzeng HT, Wang YC. Rab-mediated vesicle trafficking in cancer. J Biomed Sci 2016;23:70.
[40] Chen S, Liang MC, Chia JN, Ngsee JK, Ting AE. Rab8b and its interacting partner TRIP8b are involved in regulated secretion in AtT20 cells. J Biol Chem 2001;276:13209–16.
[41] Shen DW, Gottesman MM. RAB8 enhances TMEM205-mediated cisplatin resistance. Pharm Res 2012;29:643–50.
[42] Bravo-Cordero JJ, Marrero-Diaz R, Megias D, Genis L, Garcia-Grande A, Garcia MA, Arroyo AG, Montoya MC. MT1-MMP proinvasive activity is regulated by a novel Rab8-dependent exocytic pathway. EMBO J 2007;26:1499–510.
[43] Hattula K, Furuhjelm J, Tikkanen J, Tanhuanpaa K, Laakkonen P, Peranen J. Characterization of the Rab8-specific membrane traffic route linked to protrusion formation. J Cell Sci 2006;119:4866–77.
[44] Sopjani M, Rinnerthaler M, Almilaji A, Ahmeti S, Dermaku-Sopjani M. Regulation of cellular transport by klotho protein. Curr Protein Pept Sci 2014;15:828–35.
[45] Sorkin A, Von Zastrow M. Signal transduction and endocytosis: close encounters of many kinds. Nat Rev Mol Cell Biol 2002;3:600–14.
[46] Puisieux A, Brabletz T, Caramel J. Oncogenic roles of EMT-inducing transcription factors. Nat Cell Biol 2014;16:488–94.